Separating the Impact of Nuclear Skin and Nuclear Deformation in High-Energy Isobar Collisions

Jiangyong Jia,[1,2,*] Giuliano Giacalone,[3,†] and Chunjian Zhang[1]
[1]*Department of Chemistry, Stony Brook University, Stony Brook, New York 11794, USA*
[2]*Physics Department, Brookhaven National Laboratory, Upton, New York 11976, USA*
[3]*Institut für Theoretische Physik, Universität Heidelberg, Philosophenweg 16, 69120 Heidelberg, Germany*

(Received 7 August 2022; revised 10 June 2023; accepted 23 June 2023; published 12 July 2023)

Bulk nuclear structure properties, such as radii and deformations, leave distinct signatures in the final state of relativistic heavy-ion collisions. Isobaric collisions offer an easy route to establish explicit connections between the colliding nuclei's structure and the observable outcomes. Here, we investigate the effects of nuclear skin thickness and nuclear deformations on the elliptic flow (v_2) and its fluctuations in high-energy ^{96}Ru + ^{96}Ru and ^{96}Zr + ^{96}Zr collisions. Our findings reveal that the difference in skin thickness between these isobars only influences the inherent ellipticity of the collision systems, v_2^{rp}. In contrast, differences in nuclear deformations solely impact the fluctuations of v_2 around v_2^{rp}. Hence, we have identified a data-driven method to disentangle the effects of nuclear skin and nuclear deformations, marking a significant step toward assessing the consistency of nuclear phenomena across energy scales.

DOI: 10.1103/PhysRevLett.131.022301

The bulk properties of atomic nuclei reflect collective correlations in many-body systems held together by the strong force. Unraveling these properties and their evolution across the Segré chart constitutes a major goal in nuclear physics [1]. Traditionally, spectroscopic and scattering experiments at low energies have been employed to infer collective features of nuclei [2–4]. However, recent ultrarelativistic collision experiments have demonstrated that the dynamics of these collisions is significantly influenced by such properties [5–15]. Particularly, the angular distributions of emitted particles in high-energy collisions can be related directly to the shape of the colliding nuclei at the moment of interaction.

This connection stems from the near-ideal fluid behavior of the quark-gluon plasma (QGP) formed in high-energy collisions. In a hydrodynamic framework, anisotropies in the final-state azimuthal particle spectra emerge from spatial anisotropies in the initial conditions of the fluid expansion [16–18]. Spatial anisotropies are, in turn, sourced by the random positions of nucleons populating the colliding nuclei at the time of interaction. Unlike low-energy scattering experiments, which only provide access to average nuclear charge distributions, high-energy heavy-ion collisions can probe the spatial positions of *all* nucleons on an event-by-event basis, thus capturing multinucleon correlations. Experimental techniques employing multiparticle correlations routinely measure these correlations [19–21]. The crucial question is to what extent the established knowledge from low-energy nuclear physics can offer a coherent understanding of the phenomena observed at high-energy colliders. This Letter represents a significant step in addressing this question.

Although the influence of nuclear deformation is most pronounced in head-on collisions, it is possible to effectively isolate and study nuclear structure effects across the entire centrality range by comparing two isobaric collision systems [10,13,15]. Isobaric nuclei have the same mass number, ensuring that any differences in observables must originate from differences in their structure, which impact the initial condition and evolution of the QGP. This argument is demonstrated clearly in ^{96}Ru + ^{96}Ru and ^{96}Zr + ^{96}Zr collisions at the BNL Relativistic Heavy Ion Collider, where ratios of observables between the two systems exhibit substantial and centrality-dependent deviations from unity [22].

Most models describe the nucleon density within colliding nuclei using a Woods-Saxon (WS) profile,

$$\rho(r,\theta,\phi) \propto (1+\exp\{r-R_0[1+\beta_2 Y_2^0(\theta,\phi) + \beta_3 Y_3^0(\theta,\phi)]\}/a_0)^{-1}, \tag{1}$$

incorporating four structure parameters, nuclear skin a_0, half-width radius R_0, quadrupole deformation β_2, and octupole deformation β_3. Model studies have demonstrated that isobar ratios are indeed controlled by differences in these parameters, e.g., $\Delta\beta_2^2 = \beta_{2\mathrm{Ru}}^2 - \beta_{2\mathrm{Zr}}^2$, $\Delta\beta_3^2 = \beta_{3\mathrm{Ru}}^2 - \beta_{3\mathrm{Zr}}^2$, $\Delta a_0 = a_{0\mathrm{Ru}} - a_{0\mathrm{Zr}}$, and $\Delta R_0 = R_{0\mathrm{Ru}} - R_{0\mathrm{Zr}}$ [23].

Experimentally, many observables have been found to exhibit sensitivity to nuclear profile parameters, such as the mean transverse momentum p_T [24], its fluctuations [15], the spectator neutron number [25], flow vector correlations [26,27], and shape-size correlations [8,12,14]. In this Letter, the focus is on the elliptic flow coefficient $V_2 = v_2 e^{2i\Psi_2}$, which characterizes the quadrupole modulation of particles in the direction Ψ_2 with an amplitude v_2. V_2 emerges as a hydrodynamic response to the elliptical shape of the region of overlap between colliding nuclei. The ratio of v_2 between ^{96}Ru + ^{96}Ru and ^{96}Zr + ^{96}Zr collisions exhibits a complex nonmonotonic centrality dependence [22], which can be explained as a combined effect of the four WS parameters in Eq. (1) [28]. We show that the impact of the deformations parameters (β_2 and β_3) can be disentangled from that of the radial profile parameters (a_0 and R_0), and highlight the implications of this finding.

We begin with Fig. 1, where we represent the plane transverse to the collision axis with Cartesian coordinates, with the x direction aligned with the impact parameter direction. For events at a given centrality, the joint distribution of the real and imaginary parts of V_2, (v_{2x}, v_{2y}), approximately follows a two-dimensional Gaussian distribution [29]

$$p(v_{2x}, v_{2y}) = \frac{1}{\pi\delta^2}\exp\left[-\frac{(v_{2x} - v_2^{\rm rp})^2 + v_{2y}^2}{\delta^2}\right]. \quad (2)$$

The displacement along the x axis, $v_2^{\rm rp}$, corresponds to the reaction plane flow associated with the average elliptic geometry, whereas the fluctuation, δ, represents the variance of elliptic flow due to fluctuations in the positions of the colliding nucleons. Our argument is that changes in the radial profile of the nucleus via a_0 or R_0 modify $v_2^{\rm rp}$, while having little impact on the flow fluctuations [Fig. 1(a)]. Conversely, in the presence of nuclear deformations, the random orientation of the colliding nuclei results in an increase in δ, with little effect on $v_2^{\rm rp}$ [Fig. 1(b)] [30]. Since $p(V_2)$ is approximately Gaussian, the root-mean-squared elliptic flow is $v_2\{2\} = \sqrt{(v_2^{\rm rp})^2 + \delta^2}$, while higher-order cumulants of v_2 are all identical, $v_2\{4\} = v_2\{6\} = \ldots = v_2\{\infty\} = v_2^{\rm rp}$. In this limit, the fluctuation of v_2 can be obtained as

$$\delta^2 = v_2\{2\}^2 - v_2\{4\}^2. \quad (3)$$

In the following, we demonstrate our argument regarding the sensitivity of $v_2^{\rm rp}$ and δ to the nuclear structure parameters using transport model calculations.

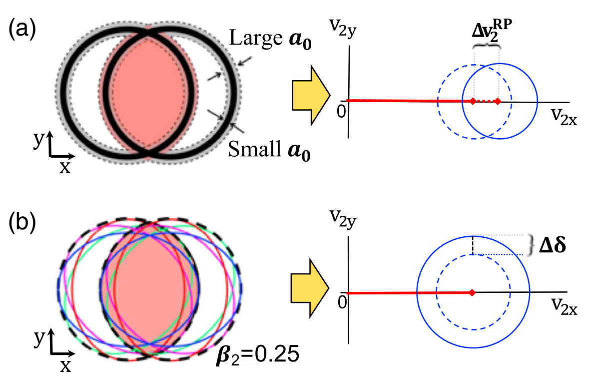

FIG. 1. (a) A schematic representation of a collision of spherical nuclei with different choices of their skin thickness, a_0. The distribution (v_{2x}, v_{2y}), denoted by blue circles, has a nonzero mean value along the x direction, $\langle v_{2x}\rangle = v_2^{\rm rp}$ indicated by red squares at the center of circles, while the variance of the distribution, corresponding to the radius of the circles, is the same along x and y. A larger skin (dashed lines) smears the elliptical shape of the QGP, resulting in a reduction of $v_2^{\rm rp}$. (b) Collisions of deformed nuclei with random orientations (four for each nucleus labeled by colored lines) would lead to an increase in the width of the distribution, denoted by δ, relative to collisions of spherical nuclei.

We simulate the dynamics of the QGP using the multiphase transport model (AMPT) [32]. Specifically, we use AMPT v2.26t5 in the string-melting mode at $\sqrt{s_{\rm NN}} = 200$ GeV with a partonic cross section of 3.0 mb [33,34]. This model has been successful in describing the isobar ratios of v_2, v_3, and $N_{\rm ch}$ measured by the STAR Collaboration [11,23]. We simulate generic isobar collisions, ^{96}X + ^{96}X, with five different choices of nuclear structure parameters β_2, β_3, R_0 and a_0, as listed in Table I. This allows us to calculate ratios that isolate the effects of these parameters step-by-step. For example, Case1 and Case2 isolate the effect of β_2, Case1 and Case3 include the effect of β_2 and β_3, and so on. We calculate the cumulants of elliptic flow within the multiparticle cumulant framework [19,20] for hadrons with $0.2 < p_T < 2$ GeV. The two-particle cumulant $v_2\{2\}$ is obtained by correlating particles in $0 < \eta < 2$ with those in $-2 < \eta < 0$ to suppress short-range correlations that do not arise from the collective expansion of the system [21]. $v_2\{4\}$, which is free from such contributions, is calculated from all particles with $|\eta| < 2$. Additionally, we calculate the true $v_2^{\rm rp}$ from the

TABLE I. Structure parameters used in the simulations of ^{96}Ru + ^{96}Ru and ^{96}Zr + ^{96}Zr collisions. Case1 and Case5 represent our full parametrizations of ^{96}Ru and ^{96}Zr, respectively.

	R_0 (fm)	a_0 (fm)	β_2	β_3
Case1 ^{96}Ru	5.09	0.46	0.162	0
Case2	5.09	0.46	0.06	0
Case3	5.09	0.46	0.06	0.20
Case4	5.09	0.52	0.06	0.20
Case5 ^{96}Zr	5.02	0.52	0.06	0.20
Ratios	(Case1/Case2), (Case1/Case3), (Case1/Case4), (Case1/Case5)			

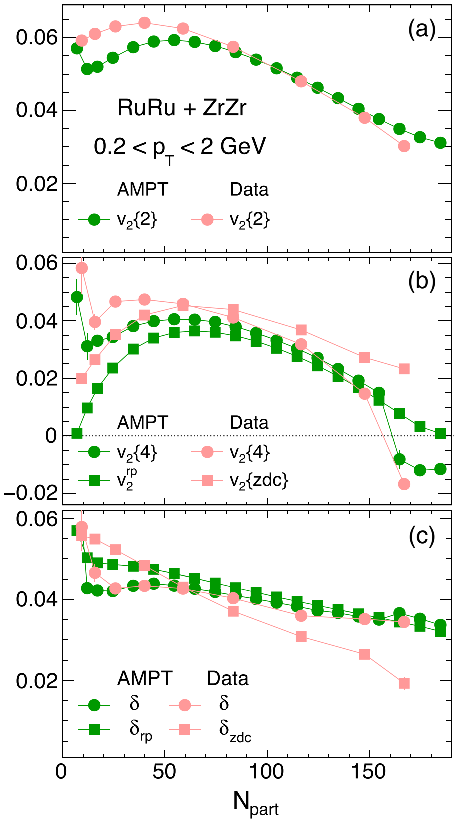

FIG. 2. Values of $v_2\{2\}$ (a), $v_2\{4\}$, and $v_2^{\rm rp}$ (b), δ and $\delta_{\rm rp}$ (c) as a function of $N_{\rm part}$, averaged between Ru + Ru and Zr + Zr collisions. The AMPT results are compared with the corresponding STAR data from Fig. 23 in Ref. [22]. For the STAR data, we approximate $v_2^{\rm rp}$ by $v_2\{\rm zdc\}$, and $\delta_{\rm rp}$ by $\delta_{\rm zdc}$, as discussed in the text.

azimuthal correlation of particles relative to the impact parameter and the true flow fluctuation $\delta_{\rm rp}$ as $\delta_{\rm rp}^2 = v_2\{2\}^2 - (v_2^{\rm rp})^2$. The simulated events are binned into classes based on the number of participating nucleons, $N_{\rm part}$.

In Fig. 2, we present our results for $v_2\{2\}$, $v_2\{4\}$, and δ, averaged over ^{96}Ru + ^{96}Ru and ^{96}Zr + ^{96}Zr collisions, which generally agree well with the STAR data. However, we note that the model underpredicts the value of $v_2\{4\}$ in off-central collisions while correctly reproducing the measured δ. This suggests that AMPT has a value of $v_2^{\rm rp}$ that is too small. This discrepancy may arise from the fact that particle production in AMPT scales with $N_{\rm part}$, which is known to lead to smaller $v_2^{\rm rp}$ compared to other models that incorporate proper energy deposition scaling [35]. Recent calculations of $v_2\{2\}$ in isobar collisions by Nijs and van der Schee using the T$_{\rm R}$ENTo model do not suffer from this issue [36].

The STAR Collaboration has also measured an approximation of $v_2^{\rm rp}$ by correlating particles with spectator neutrons in the zero-degree calorimeters (ZDC), denoted as $v_2\{\rm zdc\}$. Figure 2(b) shows that $v_2\{\rm zdc\}$ is smaller than $v_2\{4\}$ in peripheral collisions but is above it towards central collisions. The overall centrality-dependent trend is similar to that of AMPT's $v_2^{\rm rp}$, indicating that $v_2\{\rm zdc\}$ serves as a good proxy for $v_2^{\rm rp}$, at least in peripheral and midcentral collisions. In Fig. 2(c), we also define the corresponding fluctuation $\delta_{\rm zdc}$ as $\delta_{\rm zdc}^2 = v_2\{2\}^2 - (v_2\{\rm zdc\})^2$ and compare the results with the measured δ. They exhibit close agreement in peripheral collisions.

To isolate the effects of nuclear structure, we turn to isobar ratios. For an observable $\mathcal{O}$ the ratio is calculated at a given $N_{\rm part}$ as

$$R_{\mathcal{O}}(N_{\rm part}) = \frac{\mathcal{O}_{\rm Ru}(N_{\rm part})}{\mathcal{O}_{\rm Zr}(N_{\rm part})}. \quad (4)$$

Figure 3(a) shows the complex centrality dependence of $R_{v_2\{2\}}$, which arises from both deformation and radial profile parameters. In contrast, $R_{v_2\{4\}}$ in Fig. 3(b) is mainly sensitive to a_0, whereas R_δ in Fig. 3(c) is primarily sensitive to β_2 and β_3. Thus, the behavior of $R_{v_2\{2\}}$ can be decomposed into a part that is sensitive to the nuclear skin and a part that is sensitive to the nuclear deformations, supporting the intuition depicted in Fig. 1. We establish the following identity,

$$R_{v_2\{2\}}^2 = R_\delta^2 + (R_{v_2\{4\}}^2 - R_\delta^2)r, \qquad r = v_2\{4\}^2/v_2\{2\}^2, \quad (5)$$

$$R_{v_2\{2\}} \approx R_\delta + (R_{v_2\{4\}} - R_\delta)r, \quad (6)$$

where the second line is obtained by assuming all ratios are close to unity. It is known that $r \sim 0$ in central collisions, and increases to around 0.8 in mid-central collisions. Consequently, the behavior of $R_{v_2\{2\}}$ in central collisions is predominantly determined by R_δ, while the nonmonotonic behavior of $R_{v_2\{2\}}$ in midcentral collisions results from the interplay between $R_{v_2\{4\}}$ and R_δ. This constitutes our main finding.

The right column of Fig. 3 presents the ratios of the true intrinsic ellipticity, $R_{v_2^{\rm rp}}$ in Fig. 3(d), and the true flow fluctuation, $R_{\delta_{\rm rp}}$ in Fig. 3(e), obtained from $\delta_{\rm rp}^2 = v_2\{2\}^2 - (v_2^{\rm rp})^2$. We observe that, for a difference in skin thickness of $a_{0\rm Ru} - a_{0\rm Zr} = 0.06$ fm, the value of $v_2^{\rm rp}$ is enhanced by about 10% in ^{96}Ru + ^{96}Ru collisions. The impact of β_n on $R_{v_2^{\rm rp}}$ is relatively minor, as expected. Furthermore, we observe that the values of $v_2^{\rm rp}$ vary more significantly compared to $v_2\{4\}$ when structure parameters are changed. As a result, $R_{\delta_{\rm rp}}$ also exhibits a stronger dependence on these parameters than R_δ.

Note that $v_2^{\rm rp}$ and $\delta_{\rm rp}$ cannot be measured directly, and therefore the ratios of these observables are approximated by the measured $R_{v_2\{\rm zdc\}}$ in Fig. 3(d) and $R_{\delta_{\rm rp}}$ in Fig. 3(e), respectively. The STAR data agree with AMPT $R_{v_2^{\rm rp}}$ in

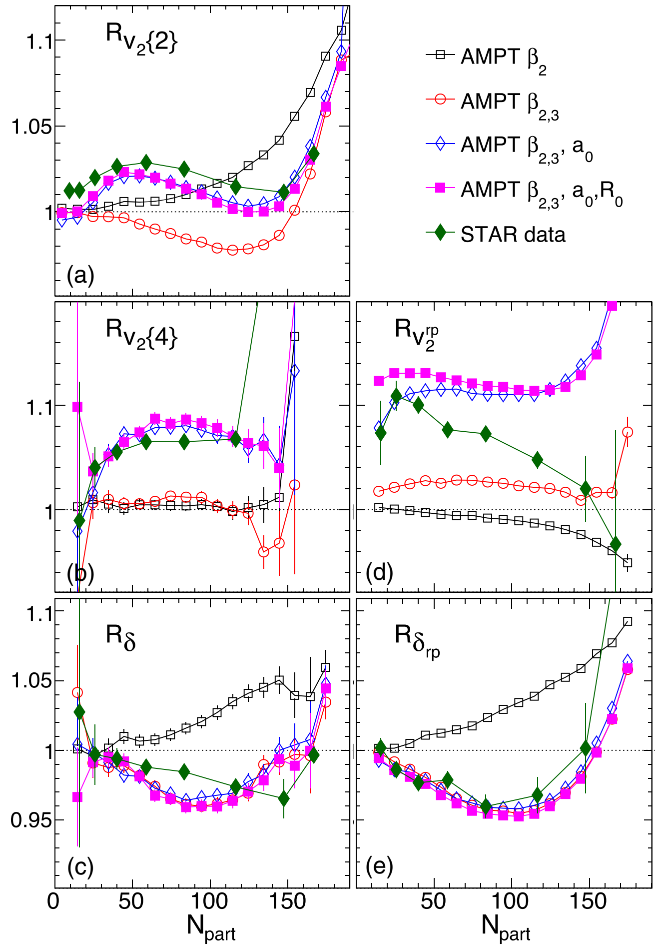

FIG. 3. Isobar ratios $R_{v_2\{2\}}$ (a), $R_{v_2\{4\}}$ (b), R_δ (c), $R_{v_2^{rp}}$ (d), and $R_{\delta_{rp}}$ (e) plotted as a function of N_{part}. For clarity and with reference to Table I, the curves labeled with β_2 correspond to Case1 and Case2, where the two nuclei differ only by their value of β_2. The curves labeled with $\beta_{2,3}$ correspond to Case1 and Case3, which includes differences in both β_2 and β_3. $\beta_{2,3}$, a_0 corresponds to Case1 and Case4, adding the difference in a_0, while $\beta_{2,3}$, a_0, R_0 corresponds to Case1 and Case5, where all Woods-Saxon parameters are different. The results are compared with STAR data from Fig. 23 of Ref. [22]. Note that v_2^{rp} and δ_{rp} cannot be measured directly, and they are approximated by STAR measurements of $v_2\{\mathrm{zdc}\}$ (d) and δ_{zdc} (e), respectively.

peripheral collisions but gradually deviate and loose sensitivity to the WS parameters in more central collisions. This discrepancy could be attributed to a strong decorrelation between the spectator plane and the reaction plane [37] when the number of spectator neutrons is small. In contrast, STAR $R_{\delta_{zdc}}$ demonstrates good agreement with AMPT $R_{\delta_{rp}}$ in Fig. 3(e).

It is worth noting that elliptic flow emerges event by event as a response to the initial ellipticity of the system, denoted by $\mathcal{E}_2$. This response follows a linear scaling, $V_2 \propto \mathcal{E}_2$ [38]. Therefore, the ratios of observables analyzed in Fig. 3 can be estimated solely based on knowledge of $\mathcal{E}_2$ and its fluctuations. In the Supplemental Material [39], we demonstrate that the observed behaviors in Fig. 3 largely originate from the initial state.

Our analysis does not rely exclusively on the Gaussian ansatz in Eq. (2) for the distribution of v_2. In fact, the fluctuations of v_2 are non-Gaussian, especially in peripheral collisions, where v_2^{rp} is large and one becomes sensitive to the bound $v_2 < 1$ [45,46]. It would be interesting to extend this study to higher-order cumulants, $v_2\{4,6,8\}$, and investigate how nuclear structure affects these quantities in isobar collisions [47]. In the Supplemental Material, we provide results for $R_{v_2\{4\}}$, $R_{v_2\{6\}}$ and $R_{v_2\{8\}}$, and also explore the fine splitting of these cumulants in terms of eccentricity fluctuations. Our preliminary findings, limited by AMPT statistics, indicate that there is no apparent separation of nuclear structure effects [39].

In summary, we have discovered that the nuclear radial profile parameters, i.e., nuclear skin thickness, a_0, and half-density radius, R_0, predominantly influence the magnitude of v_2 along the impact parameter direction captured by $v_2\{4\}$. In contrast, the nuclear deformations, β_n, primarily affect the fluctuation of elliptic flow, δ. We find that the measured isobar ratio of $v_2\{4\}$ is determined by $a_{0\mathrm{Ru}} - a_{0\mathrm{Zr}}$, while the measured isobar ratio of δ arises from the interplay between $\beta^2_{2\mathrm{Ru}} - \beta^2_{2\mathrm{Zr}}$ and $\beta^2_{3\mathrm{Ru}} - \beta^2_{3\mathrm{Zr}}$. Our results, combined with the previous finding that the isobar ratio of triangular flow is dominated by $\beta^2_{3\mathrm{Ru}} - \beta^2_{3\mathrm{Zr}}$ [23,36], provide separate constraints on three key properties of the colliding nuclei: Δa_0, $\Delta\beta_2^2$, and $\Delta\beta_3^2$.

The skin thickness as a property of the radial structure of nuclei is determined by the frame-independent one-body density of the nuclei. In contrast, deformations are defined in the intrinsic frame of nuclei and can only be captured by two- and many-body densities. Thus, separating skin and deformation effects implies that we have found an experimental method to discern the impact of one-body distribution from that of many-body correlations within nuclei. To our knowledge, such a clean separation of one-body and many-body effects is difficult to achieve in traditional low-energy nuclear structure experiments due to the larger timescales involved. Therefore, our result opens a new opportunity for nuclear structure research based on high-energy nuclear collisions.

On the side of heavy ion physics, our results can aid in the characterization of the QGP from data, which is currently limited by uncertainties in the QGP initial condition [48,49]. Reducing these uncertainties requires improving our understanding of the role of the low-energy structure of nuclei in these processes. While flow observables are very sensitive to structure parameters between isobars—up to 10% for two-particle observables [22] and even larger for higher-order correlations as seen in Fig. 2 of [50]—the influences of different structure parameters are often entangled for most observables. Our technique, which separates the effects of nuclear radial parameters from nuclear shape parameters, represents a significant step towards refining the initial condition. This reinforces the scientific case for using isobar collisions to elucidate the influence of bulk nuclear structure properties in high-energy collisions, as extensively discussed in Ref. [50]. We hope that it will stimulate further investigations using selected isobar pairs at the LHC [51].

The research of J. J and C. Z is supported by DOE DE-FG02-87ER40331. The research of G. G. is funded by the Deutsche Forschungsgemeinschaft (DFG, German Research Foundation) under Germany's Excellence Strategy EXC2181/1-390900948 (the Heidelberg STRUCTURES Excellence Cluster), within the Collaborative Research Center SFB1225 (ISOQUANT, Project-ID 273811115). We acknowledge Somadutta Bhatta and Jean-Yves Ollitrault for useful discussions.

[*]Corresponding author.
jiangyong.jia@stonybrook.edu
[†]Corresponding author.
giacalone@thphys.uni-heidelberg.de

[1] Witold Nazarewicz, Challenges in nuclear structure theory, J. Phys. G **43**, 044002 (2016).

[2] Paul E. Garrett, Magda Zielińska, and Emmanuel Clément, An experimental view on shape coexistence in nuclei, Prog. Part. Nucl. Phys. **124**, 103931 (2022).

[3] X. F. Yang, S. J. Wang, S. G. Wilkins, and R. F. Garcia Ruiz, Laser spectroscopy for the study of exotic nuclei, Prog. Part. Nucl. Phys. **129**, 104005 (2023).

[4] Bernard Frois and Costas N. Papanicolas, Electron scattering and nuclear structure, Annu. Rev. Nucl. Part. Sci. **37**, 133 (1987).

[5] Q. Y. Shou, Y. G. Ma, P. Sorensen, A. H. Tang, F. Videbæk, and H. Wang, Parameterization of deformed nuclei for Glauber modeling in relativistic heavy ion collisions, Phys. Lett. B **749**, 215 (2015).

[6] Andy Goldschmidt, Zhi Qiu, Chun Shen, and Ulrich Heinz, Collision geometry and flow in uranium + uranium collisions, Phys. Rev. C **92**, 044903 (2015).

[7] Giuliano Giacalone, Jacquelyn Noronha-Hostler, Matthew Luzum, and J. Yves Ollitrault, Hydrodynamic predictions for 5.44 TeV Xe + Xe collisions, Phys. Rev. C **97**, 034904 (2018).

[8] Giuliano Giacalone, Observing the Deformation of Nuclei with Relativistic Nuclear Collisions, Phys. Rev. Lett. **124**, 202301 (2020).

[9] Giuliano Giacalone, Constraining the quadrupole deformation of atomic nuclei with relativistic nuclear collisions, Phys. Rev. C **102**, 024901 (2020).

[10] Giuliano Giacalone, Jiangyong Jia, and Vittorio Somà, Accessing the shape of atomic nuclei with relativistic collisions of isobars, Phys. Rev. C **104**, L041903 (2021).

[11] Giuliano Giacalone, Jiangyong Jia, and Chunjian Zhang, Impact of Nuclear Deformation on Relativistic Heavy-Ion Collisions: Assessing Consistency in Nuclear Physics across Energy Scales, Phys. Rev. Lett. **127**, 242301 (2021).

[12] Jiangyong Jia, Shengli Huang, and Chunjian Zhang, Probing nuclear quadrupole deformation from correlation of elliptic flow and transverse momentum in heavy ion collisions, Phys. Rev. C **105**, 014906 (2022).

[13] Jiangyong Jia, Shape of atomic nuclei in heavy ion collisions, Phys. Rev. C **105**, 014905 (2022).

[14] Benjamin Bally, Michael Bender, Giuliano Giacalone, and Vittorio Somà, Evidence of the triaxial structure of ^{129}Xe at the Large Hadron Collider, Phys. Rev. Lett. **128**, 082301 (2022).

[15] Jiangyong Jia, Probing triaxial deformation of atomic nuclei in high-energy heavy ion collisions, Phys. Rev. C **105**, 044905 (2022).

[16] Charles Gale, Sangyong Jeon, and Bjoern Schenke, Hydrodynamic modeling of heavy-ion collisions, Int. J. Mod. Phys. A **28**, 1340011 (2013).

[17] Ulrich Heinz and Raimond Snellings, Collective flow and viscosity in relativistic heavy-ion collisions, Annu. Rev. Nucl. Part. Sci. **63**, 123 (2013).

[18] Paul Romatschke and Ulrike Romatschke, *Relativistic Fluid Dynamics In and Out of Equilibrium*, Cambridge Monographs on Mathematical Physics (Cambridge University Press, Cambridge, England, 2019).

[19] Ante Bilandzic, Raimond Snellings, and Sergei Voloshin, Flow analysis with cumulants: Direct calculations, Phys. Rev. C **83**, 044913 (2011).

[20] Ante Bilandzic, Christian Holm Christensen, Kristjan Gulbrandsen, Alexander Hansen, and You Zhou, Generic framework for anisotropic flow analyses with multiparticle azimuthal correlations, Phys. Rev. C **89**, 064904 (2014).

[21] Jiangyong Jia, Mingliang Zhou, and Adam Trzupek, Revealing long-range multiparticle collectivity in small collision systems via subevent cumulants, Phys. Rev. C **96**, 034906 (2017).

[22] Mohamed Abdallah *et al.* (STAR Collaboration), Search for the chiral magnetic effect with isobar collisions at $\sqrt{s_{NN}} =$ 200 GeV by the STAR Collaboration at the BNL relativistic heavy ion collider, Phys. Rev. C **105**, 014901 (2022).

[23] Chunjian Zhang and Jiangyong Jia, Evidence of Quadrupole and Octupole Deformations in Zr96 + Zr96 and Ru96 + Ru96 Collisions at Ultrarelativistic Energies, Phys. Rev. Lett. **128**, 022301 (2022).

[24] Hao-jie Xu, Wenbin Zhao, Hanlin Li, Ying Zhou, Lie-Wen Chen, and Fuqiang Wang, Probing nuclear structure with mean transverse momentum in relativistic isobar collisions, arXiv:2111.14812.

[25] Lu-Meng Liu, Chun-Jian Zhang, Jia Zhou, Jun Xu, Jiangyong Jia, and Guang-Xiong Peng, Probing neutron-skin thickness with free spectator neutrons in ultracentral high-energy isobaric collisions, Phys. Lett. B **834**, 137441 (2022).

[26] Shujun Zhao, Hao-jie Xu, Yu-Xin Liu, and Huichao Song, Probing the nuclear deformation with three-particle asymmetric cumulant in RHIC isobar runs, Phys. Lett. B **839**, 137838 (2023).

[27] Jiangyong Jia, Giuliano Giacalone, and Chunjian Zhang, Precision tests of the nonlinear mode coupling of anisotropic flow via high-energy collisions of isobars, Chin. Phys. Lett. **40**, 042501 (2023).

[28] Jiangyong Jia and Chunjian Zhang, Scaling approach to nuclear structure in high-energy heavy-ion collisions, Phys. Rev. C **107**, L021901 (2023).

[29] Sergei A. Voloshin, Arthur M. Poskanzer, Aihong Tang, and Gang Wang, Elliptic flow in the Gaussian model of eccentricity fluctuations, Phys. Lett. B **659**, 537 (2008).

[30] Note that changes in nuclear structure also affect the distribution $p(N_{\mathrm{part}})$, such that the events with the same N_{part} correspond to slightly different centralities and vice versa [31]. This secondary effect introduces a small correlation between $\varepsilon_2^{\mathrm{rp}}$ and β_n, but it is subleading compared to the one discussed in Fig. 1.

[31] Jiangyong Jia, Gang Wang, and Chunjian Zhang, Impact of event activity variable on the ratio observables in isobar collisions, Phys. Lett. B **833**, 137312 (2022).

[32] Zi-Wei Lin, Che Ming Ko, Bao-An Li, Bin Zhang, and Subrata Pal, A multi-phase transport model for relativistic heavy ion collisions, Phys. Rev. C **72**, 064901 (2005).

[33] Guo-Liang Ma and Adam Bzdak, Long-range azimuthal correlations in proton–proton and proton–nucleus collisions from the incoherent scattering of partons, Phys. Lett. B **739**, 209 (2014).

[34] Adam Bzdak and Guo-Liang Ma, Elliptic and Triangular Flow in $p+\mathrm{Pb}$ and Peripheral $\mathrm{Pb}+\mathrm{Pb}$ Collisions from Parton Scatterings, Phys. Rev. Lett. **113**, 252301 (2014).

[35] Giuliano Giacalone, Jacquelyn Noronha-Hostler, and J. Yves Ollitrault, Relative flow fluctuations as a probe of initial state fluctuations, Phys. Rev. C **95**, 054910 (2017).

[36] Govert Nijs and Wilke van der Schee, Inferring nuclear structure from heavy isobar collisions using Trajectum, arXiv:2112.13771.

[37] ALICE Collaboration, Elliptic flow of charged particles at midrapidity relative to the spectator plane in Pb-Pb and Xe-Xe collisions, arXiv:2204.10240.

[38] Derek Teaney and Li Yan, Triangularity and dipole asymmetry in heavy ion collisions, Phys. Rev. C **83**, 064904 (2011).

[39] See Supplemental Material at http://link.aps.org/supplemental/10.1103/PhysRevLett.131.022301 for derivation of Eq. (5) and studies based on the Glauber model, which includes Refs. [40–44].

[40] Michael L. Miller, Klaus Reygers, Stephen J. Sanders, and Peter Steinberg, Glauber modeling in high energy nuclear collisions, Annu. Rev. Nucl. Part. Sci. **57**, 205 (2007).

[41] Georges Aad *et al.* (ATLAS Collaboration), Measurement of the distributions of event-by-event flow harmonics in lead-lead collisions at = 2.76 TeV with the ATLAS detector at the LHC, J. High Energy Phys. 11 (2013) 183.

[42] Albert M. Sirunyan *et al.* (CMS Collaboration), Non-Gaussian elliptic-flow fluctuations in PbPb collisions at $\sqrt{s_{\mathrm{NN}}}=5.02$ TeV, Phys. Lett. B **789**, 643 (2019).

[43] S. Acharya *et al.* (ALICE Collaboration), Energy dependence and fluctuations of anisotropic flow in Pb-Pb collisions at $\sqrt{s_{\mathrm{NN}}}=5.02$ and 2.76 TeV, J. High Energy Phys. 07 (2018) 103.

[44] Morad Aaboud *et al.* (ATLAS Collaboration), Fluctuations of anisotropic flow in $\mathrm{Pb}+\mathrm{Pb}$ collisions at $\sqrt{s_{\mathrm{NN}}}=$ 5.02 TeV with the ATLAS detector, J. High Energy Phys. 01 (2020) 051.

[45] Giuliano Giacalone, Li Yan, Jacquelyn Noronha-Hostler, and J. Yves Ollitrault, Skewness of elliptic flow fluctuations, Phys. Rev. C **95**, 014913 (2017).

[46] Rajeev S. Bhalerao, Giuliano Giacalone, and Jean-Yves Ollitrault, Kurtosis of elliptic flow fluctuations, Phys. Rev. C **99**, 014907 (2019).

[47] Giuliano Giacalone, Elliptic flow fluctuations in central collisions of spherical and deformed nuclei, Phys. Rev. C **99**, 024910 (2019).

[48] D. Everett, W. Ke, J. F. Paquet, G. Vujanovic, S. A. Bass *et al.* (JETSCAPE Collaboration), Multisystem Bayesian constraints on the transport coefficients of QCD matter, Phys. Rev. C **103**, 054904 (2021).

[49] Govert Nijs, Wilke van der Schee, Umut Gürsoy, and Raimond Snellings, Transverse Momentum Differential Global Analysis of Heavy-Ion Collisions, Phys. Rev. Lett. **126**, 202301 (2021).

[50] Benjamin Bally *et al.*, Imaging the initial condition of heavy-ion collisions and nuclear structure across the nuclide chart, arXiv:2209.11042.

[51] Z. Citron *et al.*, Report from Working Group 5: Future physics opportunities for high-density QCD at the LHC with heavy-ion and proton beams, CERN Yellow Rep. Monogr. **7**, 1159 (2019).